AIP Advances

Induced conductivity in sol-gel ZnO films by passivation or elimination of Zn vacancies

Cite as: AIP Advances **6**, 095004 (2016); https://doi.org/10.1063/1.4962658
Submitted: 19 November 2015 • Accepted: 29 August 2016 • Published Online: 08 September 2016

D. J. Winarski, W. Anwand, A. Wagner, et al.

ARTICLES YOU MAY BE INTERESTED IN

Positron annihilation lifetime and Doppler broadening spectroscopy at the ELBE facility
AIP Conference Proceedings **1970**, 040003 (2018); https://doi.org/10.1063/1.5040215

Electrical, optical and structural properties of transparent conducting Al doped ZnO (AZO) deposited by sol-gel spin coating
AIP Advances **8**, 065307 (2018); https://doi.org/10.1063/1.5023020

A comprehensive review of ZnO materials and devices
Journal of Applied Physics **98**, 041301 (2005); https://doi.org/10.1063/1.1992666

AIP Advances
Mathematical Physics Collection
READ NOW

AIP Publishing

© 2016 Author(s).

AIP ADVANCES **6**, 095004 (2016)

Induced conductivity in sol-gel ZnO films by passivation or elimination of Zn vacancies

D. J. Winarski,[1] W. Anwand,[2] A. Wagner,[2] P. Saadatkia,[1] F. A. Selim,[1,a] M. Allen,[3] B. Wenner,[4] K. Leedy,[4] J. Allen,[3] S. Tetlak,[4] and D. C. Look[4]
[1]*Department of Physics and Astronomy, Bowling Green State University, Bowling Green, Ohio 43403, USA*
[2]*Institute of Radiation Physics, Helmholtz-Zentrum Dresden-Rossendorf, Bautzner Landstr. 400, 01328 Dresden, Germany*
[3]*Air Force Research Laboratory, Munitions Directorate, Eglin AFB, FL 32542, USA*
[4]*Air Force Research Laboratory Sensors Directorate, Wright-Patterson Air Force Base, Ohio, 45431, USA*

(Received 19 November 2015; accepted 29 August 2016; published online 8 September 2016)

Undoped and Ga- and Al- doped ZnO films were synthesized using sol-gel and spin coating methods and characterized by X-ray diffraction, high-resolution scanning electron microscopy (SEM), optical spectroscopy and Hall-effect measurements. SEM measurements reveal an average grain size of 20 nm and distinct individual layer structure. Measurable conductivity was not detected in the unprocessed films; however, annealing in hydrogen or zinc environment induced significant conductivity ($\sim 10^{-2}$ Ω.cm) in most films. Positron annihilation spectroscopy measurements provided strong evidence that the significant enhancement in conductivity was due to hydrogen passivation of Zn vacancy related defects or elimination of Zn vacancies by Zn interstitials which suppress their role as deep acceptors. Hydrogen passivation of cation vacancies is shown to play an important role in tuning the electrical conductivity of ZnO, similar to its role in passivation of defects at the Si/SiO2 interface that has been essential for the successful development of complementary metal–oxide–semiconductor (CMOS) devices. By comparison with hydrogen effect on other oxides, we suggest that hydrogen may play a universal role in oxides passivating cation vacancies and modifying their electronic properties. © *2016 Author(s). All article content, except where otherwise noted, is licensed under a Creative Commons Attribution (CC BY) license (http://creativecommons.org/licenses/by/4.0/).* [http://dx.doi.org/10.1063/1.4962658]

I. INTRODUCTION

Transparent conductive oxides (TCO) have many applications such as transparent electrodes, window metals in light emitting diodes, flat panel displays, sensors, plasmonics and solar cells.[1] ZnO has emerged as a promising material to replace indium tin oxide (ITO),[2] the dominant TCO in most applications. Several contributing factors have led to the interest in ZnO including high cost of ITO and limiting supply of indium. ZnO, on the other hand, is a nontoxic material and can be easily grown[3,4] using standard techniques such as sputtering, pulsed laser deposition (PLD) and sol-gel as demonstrated in this letter. Highly transparent conductive ZnO films can be obtained by doping ZnO with group-III metals such as Al and Ga. They have loosely bound valence electrons, which can be excited beyond the conduction band minimum at room temperature. Al- and Ga- ZnO films grown by PLD, molecular beam epitaxay and chemical vapor deposition methods have shown carrier concentrations on the order of 10^{20} cm^{-3}.[4,5] Various wet chemistry coating techniques[6–10] have also been applied to synthesize ZnO thin films, but high levels of intrinsic defects make it difficult to control the film

[a]Corresponding author: faselim@bgsu.edu

 © Author(s) 2016

properties. Despite considerable research on sol-gel ZnO films, no detailed structural information on film layering, thickness uniformity, and defect nature are available. In this work we use the sol-gel and spin coating method[7–11] to synthesize ZnO films and introduce in them extrinsic shallow donors such as Al^{3+} and Ga^{3+} through precursor solutions, followed by various post processing heat treatment techniques to tune the film properties. Group III elements such as Al^{3+} and Ga^{3+} have similar ionic radius to that of Zn^{2+} and thus can easily replace it with little effect on the lattice structure.[8,12,13] The characterization section of the article focuses on relating the electrical properties of the fabricated films to their atomic structures and defects using data obtained from high resolution scanning electron microscopy (SEM) and positron annihilation spectroscopy (PAS) techniques.[14] The Doppler broadening of positron annihilation (DBPA) measurements presented in this work reveal strong passivation of Zn vacancy related defects by hydrogen that immensely alters the electrical conductivity of the films. Although the enhancement in the conductivity of ZnO by hydrogen anneals has been reported for films grown by different methods,[15] the reason behind it is not understood. A few works have suggested that the enhancement in conductivity may be due to desorption of negatively charged oxygen species from the grain boundary surfaces.[15–17] We show in this work that hydrogen passivation of Zn vacancy related defects may be also behind the enhancement in conductivity in the studied films as evident from PAS measurements. Hydrogen passivation of defects has been recognized to be the major factor in the successful development of complementary metal-oxide-semiconductor devices.[18–20] Recent works by one of the authors have also demonstrated that hydrogen passivate cation vacancies in yttrium aluminum oxide $Y_3Al_5O_{12}$ and dramatically modified its optical and electronic properties.[21,22] The current work shows that hydrogen passivates Zn vacancy related defects and plays an important role in tuning the electrical properties of ZnO films as well. We suggest that hydrogen may play a universal role in oxides passivating cation vacancies and modifying their electronic properties.

II. EXPERIMENTAL DETAILS AND MEASUREMENTS

Film synthesis: A precursor solution was made using 2-methoxyethanol and ethanolamine (MEA) as a solvent and stabilizer, respectively. High purity zinc acetate was dissolved at a 1:1 molar ratio with MEA to obtain a 0.75M transparent homogeneous solution. High purity aluminum nitrate nonahydrate and gallium nitrate hydrate salts were added to obtain a doping level of 1- 3% in solution. The prepared solutions were heated to 60°C, stirred for 2 hours, and cooled to room temperature prior to spin coating onto 1 inch diameter quartz substrates. To improve solution/substrate compatibility, the substrates were treated in a series of piranha etching baths. The substrate was placed in a 3:1 H_2SO_4:H_2O_2 bath at 80°C for 15 minutes, then rinsed with deionized (DI) water, and placed in a 3:1 NH_4OH:H_2O_2 bath at 80°C for 15 minutes, rinsed with DI water again, and placed in an oven at about 100°C to dry. During spin coating, the substrate spins at 500 rpm, where 40-50 drops of precursor solution were dispensed in 15 seconds. The deposited film and substrate were then spun at 3000 rpm for 30 seconds to obtain an amorphous transparent gel-like thin layer. Next, the deposited film on the substrate was placed in an oven to dry at 150°C for 10 minutes. The spin coating and drying processes were repeated to obtain the desired number of layers. Finally, the films were annealed

TABLE I. Hall Effect measurements for doped and undoped ZnO thin films grown by sol-gel spin coating. It lists the film type and thickness, resistivity, carrier concentration, and mobility. The thicknesses of the films were evaluated from ellipsometry and SEM measurements. The low values of electron mobility are due to inaccuracy in their measurements.

	thickness (cm)	Resistivity (ohm cm)	mobility (cm^2/V s)	Concentration (cm^{-3})
1% Ga:ZnO 14layers in h2 1hr	8.00E-05	1.03E+01	0.0425	1.43E+19
1% Ga:ZnO 14layers in h2 1 hr, Zn 1hr	8.08E-05	1.97E-01	0.221	1.44E+20
1% Al:ZnO 16layers in h2 1hr, Zn 1hr, Zn 3 hrs	5.15E-05	1.71E-02	0.121	3.01E+21
ZnO 10 layers in H2/N2 1hr, Zn 3 hrs	6.00E-05	1.83E-01	29.4	1.16E+18
ZnO 12 layers in Zn 1 hr	1.73E-05	1.08E+02	0.31	1.86E+17

in ambient air at 400°C for 1 hour, which is essential to obtain the ZnO structure. In an effort to tune the electronic properties, a number of samples were further annealed in various atmospheres under the following conditions: 1- forming gas of 95%N_2 and 5% H_2 at 400°C for 1 hr, 2- H_2 flow at 400°C for 1 hr, 3- Zn-rich environment at 400°C for 1 hr. Zn-rich environment was created

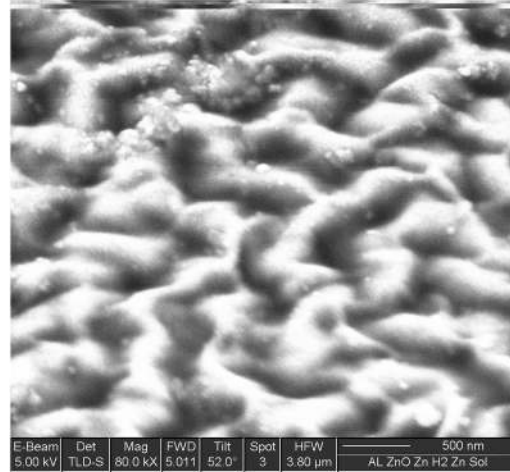

(a)

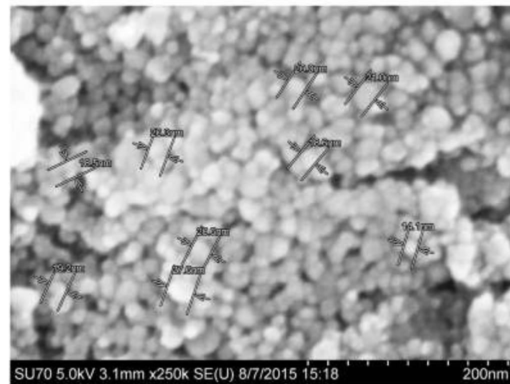

(b)

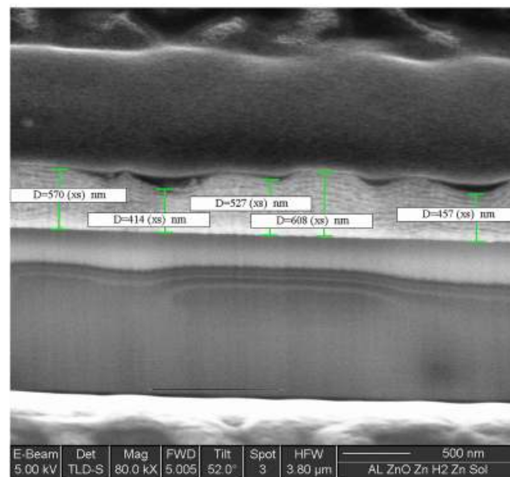

(c)

FIG. 1. SEM images for 1% Al:ZnO film annealed first in H_2 flow and later in Zn-rich environment.

by wrapping films in pure Zn foil filled with Zn powder while flowing N_2 or Ar gas to prevent oxidation.

The crystallographic nature and morphology of the films were investigated by X-ray diffraction (XRD) and high resolution scanning electron microscopy (SEM). Focused ion beam was employed in conjunction with SEM to obtain high resolution cross sectional images. The thicknesses of the films were evaluated from ellipsometry measurements and SEM images and are presented in Table I. Optical absorption spectra were recorded at room temperature using a double beam Perkin Elmer UV-VIS-NIR spectrometer from 190 to 1100 nm. Two probe measurements were first carried out to check the film conductivity; then the resistivity, carrier concentration, and mobility were evaluated from room temperature van der Pauw Hall-effect measurements.

Depth-resolved Doppler broadening of PAS measurements were performed at the positron facility at Helmholtz-Zentrum Dresden-Rossendorf (HZDR) in Dresden, Germany using monoenergetic positron beams from 0.2 keV to 30 keV. The 511 KeV annihilation peak was recorded using a high purity Ge detector at each beam energy. The Doppler broadening was then characterized by the S and W parameters[14] as explained below.

III. RESULTS AND DISCUSSION

A. Structural characterization

High-resolution SEM images for 1% Al doped ZnO film annealed in both H_2 and Zn environments after air anneal are shown in Fig. 1. The lower magnification images show worm like structures (Fig. 1a), and at higher magnification round particles with average particle size of 20 nm (Fig. 1b). A high resolution cross-section image for the film is presented in Fig. 1c; it reveals that the film is deposited as distinct individual layers (each layer is ~40 nm thick). The image also reveals non-uniform thickness, with ~25% variation across the film and indicates that it is difficult to obtain uniform thickness using sol-gel methods. We are not aware of any previous high-resolution cross section images for sol-gel films. According to the current measurements we anticipate that the distinct individual layers and the non-uniformity in thickness are inherent of the sol-gel method, but they may be reduced by further annealing. As shown below none of them hinders the electrical properties of the films. The distinct individual layers, however, lead to interference effects as shown below in the optical transmission spectra.

Figure 2 shows the XRD spectra for Al:ZnO films annealed in various ambient conditions. The XRD pattern indicates that the films are polycrystalline; and shows diffraction peaks belonging

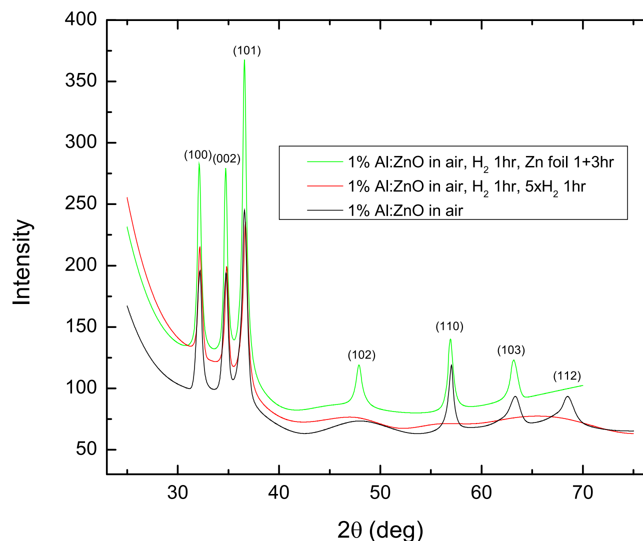

FIG. 2. XRD measurements for Al:ZnO films annealed in various atmospheres.

to (100), (002), and (101) planes in all films. All observed diffraction peaks match the hexagonal wurtzite ZnO structure indicating the absence of any secondary phases in the films. XRD spectra were also measured for undoped ZnO films (not shown in the figure) and compared with the spectra for Al doped films. The comparison illustrated that the peaks of the diffraction pattern of Al doped films are slightly shifted to right (0.3 degree increase in angle). This indicates that Al incorporation induces small variation in the lattice constant parameters. Annealing in Zn ambient enhances the polycrystalline nature of the film, while annealing in H_2 flow for 2 hours leads to an opposite effect.

B. Optical and electrical characterization

Optical transmission measurements displayed in Fig. 3 show the band gap edge of ZnO and indicate that the films are highly transparent in the visible range. The individual layers observed within the film from SEM images lead to interference effects as shown in the optical spectra. Annealing

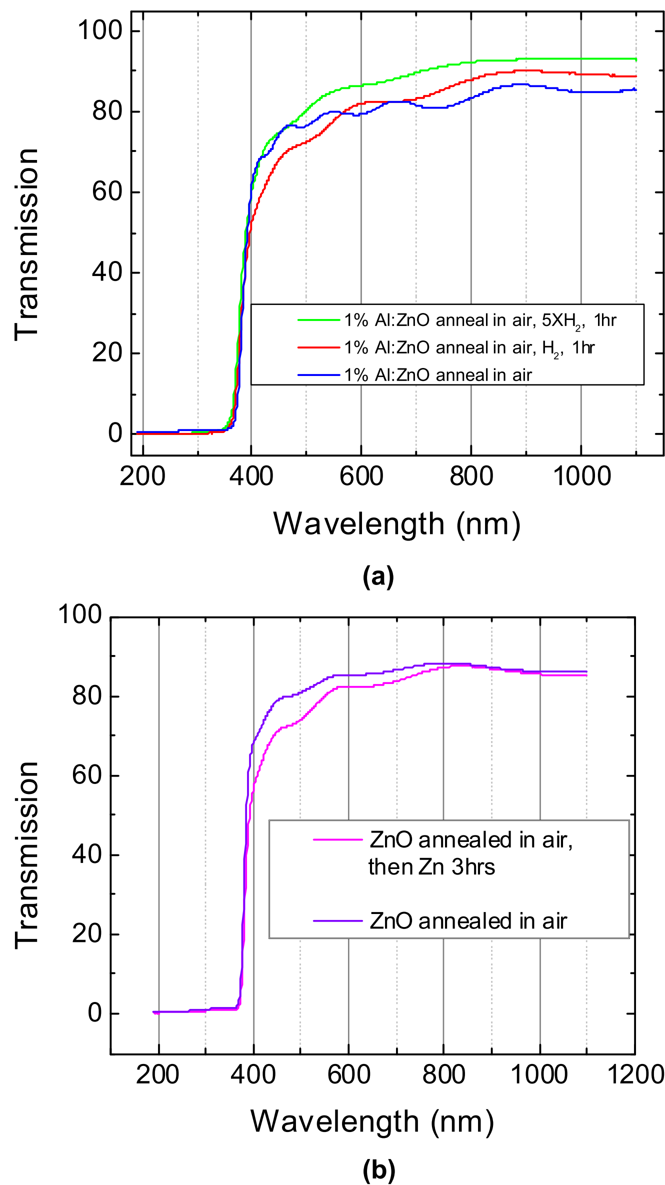

FIG. 3. Optical transmission measurements for: (a) Al:ZnO films before and after hydrogen treatment, (b) undoped ZnO before and after Zn treatment.

in H_2 for longer durations has minimized interference (Fig. 3(a)), which may be an indication for better overlapping of layers after anneal. Film transparency was also improved after hydrogen anneal. However, this is not the case after Zn ambient anneals (Fig. 3(b)), which promoted polycrystallinity.

Two-probe measurements showed no measurable conductivity in all as-grown and air-annealed undoped and doped ZnO films. However, a large conductivity has been induced in the films after H_2 or Zn anneal. Hall Effect measurements on films annealed in different environments are summarized in Table I. The lowest electrical resistivity ($1\text{x}10^{-2}\Omega$.cm) and highest carrier concentration were measured in Al-doped ZnO after both H_2 and Zn anneals. We emphasize that all the undoped and

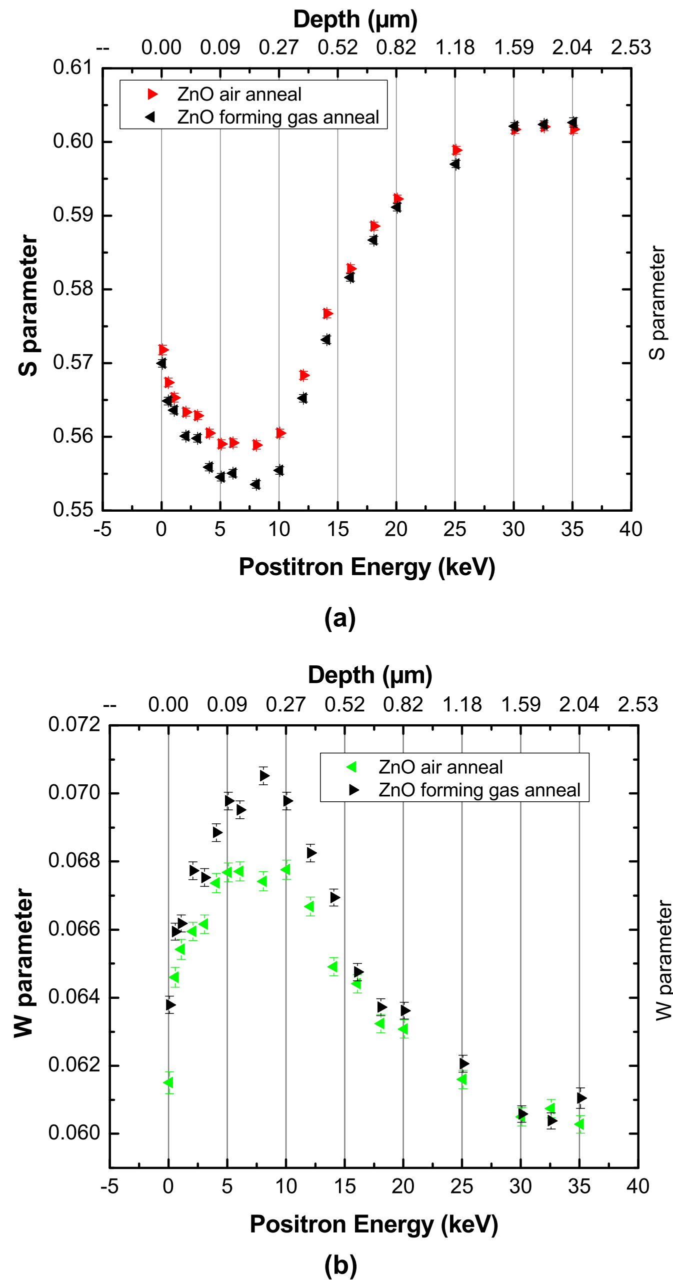

FIG. 4. Depth resolved positron annihilation spectroscopy for Al:ZnO before and after forming gas (H_2 + N_2) anneal: (a) S-parameter as a function of positron beam energy and mean positron implantation depth, (b) W-parameter as a function of positron beam energy and mean positron implantation depth.

doped ZnO films were highly resistive before H_2 or Zn anneal. It is well understood that Al and Ga add donors to ZnO, however, significant conductivity is only induced after those anneals.

C. Positron annihilation spectroscopy

Depth-resolved Doppler broadening of PAS measurements were applied to elucidate the effect of annealing as PAS is well suited to identify neutral or negatively charged vacancy type defects in semiconductors and oxides.[14,23–26] Because of the lack of positive ion cores, vacancies form an attractive potential that traps positrons leading to characteristic changes in the measured positron annihilation parameters. Many works have applied PAS and identified Zn vacancies in ZnO films and bulk single crystals.[24–26] Here, the measurements were carried on Al:ZnO films before and after annealing in forming gas of H_2 and N_2. Figures 4(a) and (b) show S and W parameters for the two films as a function of incident positron energy and mean implantation depth. The S and W parameters[27–29] represent the annihilation fraction of positrons with valence and core electrons respectively and they provide an indication about defect density. S was obtained from the 511 keV peak by dividing the counts in the central peak by the total counts in the peak while W was obtained by dividing the counts in the wings of the peak by the total counts in the peak. Trapped positrons at defects are more likely to annihilate with low momentum valence electrons causing an increase in S parameter and a decrease in W parameter.[27–29] In Fig. 4(a) and (b), the S parameter shows a relatively higher value and the W-parameter shows a relatively lower value at low positron energy (0- 5) keV, which is due to positron annihilation at the surface of the films. The graphs show a significant decrease in S parameter and increase in W parameter after H_2-anneal which can be interpreted ae follows. A Zn vacancy with its negative charge state is an effective trapping center for positrons while O vacancy or interstitial defects cannot trap positrons. Therefore the decrease of S-parameter and increase of W parameter after H_2-anneal is an obvious indication of the reduction or passivation of Zn vacancy related defects. Annealing in forming gas of H_2 and N_2 cannot eliminate Zn vacancies, however hydrogen can partially or completely fill Zn vacancies modifying their negative charge state, which prevents positron trapping. Zn interstitials can also fill Zn vacancies and prevent positron trapping. Figure 5 presents the S versus W parameters plot for ZnO films after air anneal, ZnO films after forming gas anneal and ZnO bulk single crystals. The points on the graph represent the data points corresponding to energy values at which positrons annihilate only in the middle of the film without any influence from the surface or the substrate. The line in the S versus W plot runs through the bulk value, which is an indication that there is only one dominant defect type in the samples.[14,28] This illustrates that H_2 anneal did not create new defect but only reduced Zn vacancies, the dominant

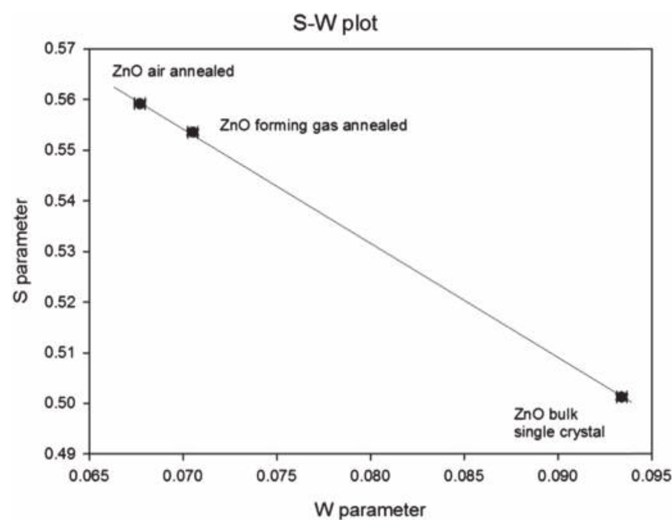

FIG. 5. S versus W graph for bulk ZnO single crystal and Al:ZnO films before and after forming gas (H_2 + N_2) anneal. The three points lie on straight line indicting one dominant defect type.

trapping defect for positrons in ZnO. These measurements showed that Zn vacancy related defects are dominant in sol-gel ZnO films and provided strong evidence that hydrogen passivates Zn vacancies eliminating their deep acceptor state which leads to a large increase in carrier concentration and induce high conductivity in the films. Improving the electrical conductivity of sol-gel ZnO films is crucial for its applications as TCO.[30–35]

IV. CONCLUSIONS

In conclusion, ZnO films doped with Al and Ga were synthesized using sol-gel and spin coating methods. XRD analysis showed that the films are polycrystalline and do not contain secondary phases and High-resolution cross section SEM measurements revealed individual layered structure and nonuniform thickness with 25% variation. The individual layering is expected to be characteristic of the sol-gel growth, however it does not seem to have a significant effect on the electrical properties. Measurable conductivity was only induced in the films after annealing in H_2 or Zn environments. This dramatic effect of post thermal treatments was studied by PAS which revealed a significant decrease in the concentration of Zn vacancies. This could be due to filling of Zn vacancies by Zn interstitials or their passivation by hydrogen which modifies their negative charge state and eliminates their role as deep acceptors. This work demonstrates the role of Zn vacancies in suppressing the n-conductivity. It also shows the significant role that hydrogen passivation of cation vacancies play in ZnO and its immense effects on the electrical properties. This is consistent with the role of hydrogen passivation of cation vacancies that has been reported in a few semiconducting and dielectric oxides. We suggest that hydrogen plays a universal role in oxides passivating their cation vacancies and modifying their electronic properties.

ACKNOWLEDGMENTS

The authors would like to thank Timothy Cooper and Wallace Rice at Air Research laboratory for their contributions. Funding for this work was provided by AFRL/DAGSI project RY14.

[1] A. Stadler, Materials **5**, 661 (2012).
[2] H. Li, L. K. Schirra, J. Shim, H. Cheun, B. Kippelen, O. L. A. Monti, and J.-L. Bredas, Chem. Mater. **24**(15), 3044 (2012).
[3] D. C. Look, Mater. Sci. Eng. B **80**, 383 (2001).
[4] J. Hu and R. G. Gordon, J. Appl. Phys. **71**, 880 (1992).
[5] H. J. Ko, Y. F. Chen, S. K. Hong, H. Wenisch, T. Yao, and D. C. Look, Appl. Phys. Lett. **77**, 3761.
[6] W. J. Chen, W. L. Liu, S. H. Hsieh, and Y. G. Hsu, Procedia Engineering **36**, 54–61 (2012).
[7] M. R. Alfaro Cruz, G. Ortega Zarzoza, G. A. Martinez Castanon, and J. R. Martinez, *Current Microscopy Contributions to Advances in Science and Technology* (A. Mendez Villas Ed.) 1370-1376 (2012).
[8] L. Znaidi, T. Touman, D. Vrel, N. Souded, S. B. Yahia, O. Brinza, A. Fischer, and A. Boudrioua, Coatings **3**, 126–139 (2013).
[9] K. L. Foo, M. Kashifi, U. Hashim, and M. E. Ali, Current Nanoscience **9** (2013).
[10] S. Salam, M. Islam, and A. Akram, Thin Solid Films **529**, 242–247 (2013).
[11] S. A. Kamauddin, K. Y. Chan, H. K. Yow, M. Z. Sahdan, H. Saim, and D. Knipp, Appl. Phys. A **104**(1), 263–268 (2010).
[12] Y. Liu, Y. Li, and H. Zeng, Journal of Nanomaterials **2013**, 196521 (2013).
[13] F. H. Wang, C. T. Chou, T. K. Kang, and C. C. Huang, Journal of Ceramic Processing Research **14**, 149–152 (2013).
[14] R. Krause-Rehberg and H. Leipner, *Positron Annihilation in Semiconductors* (Springer-Verlag, 1999).
[15] B. Oh, M. Jeong, D. Kim, W. Lee, and J. Myoung, Journal of Crystal Growth **281**, 475 (2005).
[16] K. Zhang, F. Zhu, C. H. A. Huan, and A. T. S. Wee, J. Appl. Phys. **86**, 974 (1999).
[17] B. Theys, V. Sallet, F. Jomard, A. Lusson, J. F. Rommeluere, and Z. Teukam, J. Appl. Phys. **91**, 3922 (1997).
[18] P. C. Srivastava and U. P. Singh, Bull. Mater. Sci. **19**, 51 (1996).
[19] C. G. Van de Walle and J. Neugebauer, Ann. Rev. Mater. Res. **36**, 179 (2006).
[20] C. G. Van de Walle, IEEE Trans. Electron Devices **47**, 1779 (2000).
[21] F. A. Selim, C. Varney, M. C. Taurn, M. Rowe, G. S. Collins, and M. D. McCluskey, Phys. Rev. B **88**, 174102 (2013).
[22] D. Winarski, C. Persson, and F. A. Selim, Appl. Phys. Lett. **105**, 041102 (2014).
[23] F. A. Selim, D. Winarski, C. R. Varney, M. C. Tarun, J. Ji, and M. D. McCluskey, Results in Physics **5**, 28 (2015).
[24] J. Čížek, J. Valenta, P. Hruška, O. Melikhova, I. Procházka, M. Novotný, and J. Bulíř, Appl. Phys. Lett. **106**, 251902 (2015).
[25] L. J. Brillson, Z. Zhang, D. R. Doutt, D. C. Look, B. G. Svensson, A. Yu. Kuznetsov, and F. Tuomisto, Physica Status Solidi B **250**, 1953 (2013).
[26] F. A. Selim, M. H. Weber, D. Solodovnikov, and K. G. Lynn, Phys. Rev. Lett. **99**(8), 085502 (2007).
[27] P. Hautojaervi, *Positrons in Solids* (Springer-Verlag, Heidelberg, 1979).
[28] P. Schultz and K. G. Lynn, Rev. Mod. Phys. **60**, 701 (1988).
[29] F. A. Selim, D. P. Wells, J. F. Harmon, and J. Williams, J. Appl. Phys. **97**, 113539 (2005).

[30] M. Chen, Z. L. Pei, C. Sun, J. Gong, R. F. Huang, and L. S. Wen, Mat. Sci. and Eng. B-Solid **85**, 212 (2001).
[31] P. R. Chalker, P. A. Marshall, S. Romani, J. W. Roberts, S. J. C. Irvine, D. A. Lamb, A. J. Clayton, and P. A. Williams, J. Vac. Sci. Technol. A **31**, 01A120 (2013).
[32] J. K. Srivastava, L. Agrawal, and B. Bhattacharyya, J. Electrochem. Soc. **136**(11), 3414 (1989).
[33] K. Hazra and S. Basu, Solid State Electron. **49**(7), 1158 (2005).
[34] K. L. Chopra, S. Major, and D. K. Pandya, Thin Solid Films **102**, 1 (1983).
[35] H. Li, L. K. Schirra, J. Shim, H. Cheun, B. Kippelen, O. L. A. Monti, and J. L. Bredas, Chem. Mater. **24**, 3044 (2012).